Available online at www.sciencedirect.com
ScienceDirect
Carbon 44 (2006) 2715–2723
CARBON
www.elsevier.com/locate/carbon

Adsorption and electrothermal desorption of organic vapors using activated carbon adsorbents with novel morphologies

Lingai Luo [a,*], David Ramirez [b], Mark J. Rood [b,e,*], Georges Grevillot [c], K. James Hay [d], Deborah L. Thurston [b,e]

[a] LOCIE, ESIGEC, Universite de Savoie, Campus Scientific, Savoie Technolac, 73376, Le Bourget-Du-Lac cedex, France
[b] Department of Civil and Environmental Engineering, University of Illinois, Urbana, IL 61801-2352, USA
[c] Laboratoire des Sciences du Genie Chimique, CNRS, ENSIC-INPL, BP451 54001, Nancy, France
[d] U.S. Army Engineer Research and Development Center, Construction Engineering Research Laboratory, Champaign, IL 61826-9005, USA
[e] Department of General Engineering, University of Illinois, Urbana, IL 61801-2352, USA

Received 22 January 2006; accepted 3 April 2006
Available online 5 June 2006

Abstract

Novel morphologies of activated carbons such as monolith, beads and fiber cloth can effectively capture organic vapors from industrial sources. These adsorbent materials are also unique because they can undergo direct electrothermal regeneration to recover the adsorbed organic vapors for potential re-use. This investigation compares and contrasts the properties of these adsorbents when using electrothermal–swing adsorption. The adsorption systems consisted of an organic vapor generation system, an electrothermal–swing adsorption vessel, a gas detection unit, and a data acquisition and control system. The activated carbon monolith (ACM) had the lowest pressure drop, highest permeability, highest electrical resistivity and lowest cost as compared to the activated carbon beads (ACB) and the activated carbon fiber cloth (ACFC). ACB had the largest throughput ratio and lowest length of unused bed as compared to the other adsorbents. However, ACFC had the largest adsorption capacity for toluene when compared to ACM and ACB. ACFC was also faster to regenerate and had a larger concentration factor than ACM and ACB. These results describe relevant physical, electrical, adsorption and cost properties for specific morphologies of the adsorbents to more effectively capture and recover organic vapors from gas streams.

Keywords: Activated carbon; Carbon beads; Carbon cloth; Adsorption; Adsorption properties

1. Introduction

Adsorption processes with activated carbons are widely used to remove organic vapors from gas streams that are generated from a wide range of industries. Methods used to regenerate carbonaceous adsorbents include steam [1,2], warm dry gas [3,4], vacuum [5], and indirect [6,7]/direct [8] electrothermal treatments. Regeneration of these activated carbons results in gas streams that contain concentrated single component or multi-component organic compounds. These concentrated compounds are then more readily destroyed or recovered before they are emitted to the atmosphere. Destruction of the organic vapors generally occurs by incineration or biofiltration. Recovery of the organic vapors as liquids typically occurs for industrial gas streams by condensation and possibly phase separation. This paper discusses the adsorption of organic vapors and direct electrothermal regeneration with activated carbon adsorbents in the form of a monolith, beads and fiber cloth.

Direct-electrothermal regeneration by the direct Joule effect uses the adsorbent as an electrical resistor to heat

* Corresponding authors. Tel.: +1 4 79 75 81 93; fax: +1 4 79 75 81 44 (L. Luo), tel.: +1 217 333 6963; fax +1 217 333 6968 (M.J. Rood)
E-mail addresses: Lingai.LUO@univ-savoie.fr (L. Luo), mrood@uiuc.edu (M.J. Rood).

0008-6223/$ - see front matter © 2006 Elsevier Ltd. All rights reserved.
doi:10.1016/j.carbon.2006.04.007

Report Documentation Page

Form Approved
OMB No. 0704-0188

1. REPORT DATE	2. REPORT TYPE	3. DATES COVERED
2006		**00-00-2006 to 00-00-2006**

4. TITLE AND SUBTITLE	5a. CONTRACT NUMBER
Adsorption and Electrothermal Desorption of Organic Vapors Using Activated Carbon Adsorbents With Novel Morphologies	5b. GRANT NUMBER
	5c. PROGRAM ELEMENT NUMBER
6. AUTHOR(S)	5d. PROJECT NUMBER
	5e. TASK NUMBER
	5f. WORK UNIT NUMBER
7. PERFORMING ORGANIZATION NAME(S) AND ADDRESS(ES) **LOCIE, ESIGEC,,Universite de Savoie, Campus Scientific, Savoie Technolac,73376, Le Bourget-Du-Lac cedex, France, ,**	8. PERFORMING ORGANIZATION REPORT NUMBER
9. SPONSORING/MONITORING AGENCY NAME(S) AND ADDRESS(ES)	10. SPONSOR/MONITOR'S ACRONYM(S)
	11. SPONSOR/MONITOR'S REPORT NUMBER(S)

12. DISTRIBUTION/AVAILABILITY STATEMENT
Approved for public release; distribution unlimited

13. SUPPLEMENTARY NOTES
U.S. Government or Federal Rights.

14. ABSTRACT

15. SUBJECT TERMS

16. SECURITY CLASSIFICATION OF:			17. LIMITATION OF ABSTRACT	18. NUMBER OF PAGES	19a. NAME OF RESPONSIBLE PERSON
a. REPORT **unclassified**	b. ABSTRACT **unclassified**	c. THIS PAGE **unclassified**	**Same as Report (SAR)**	**9**	

and regenerate the adsorbent. Alternating or direct current can be used to heat and regenerate the adsorbent. The use of direct-electrothermal regeneration as part of an electrothermal–swing adsorption system has been used to regenerate activated carbon fiber cloth (ACFC) that contained tricholoroethane [8], ACFC that contained a range of compounds including ethanol and ethyl acetate [9,10], ACFC that contained a wide range of alkanes, aromatics, and ketone containing organic vapors [11–13], and activated carbon monolith [14]. The redistribution of adsorbed VOCs in activated carbon during direct-electrothermal regeneration was also studied [15]. Regeneration of activated carbon by direct-electrothermal heating avoids the introduction of water into the adsorption vessel, and the electrical power that is used to heat the adsorbent is controlled independent of the carrier gas flow rate. Independent control of the heating rate and carrier gas flow rate allows careful control the adsorbent's temperature and the rate of desorption for the organic vapor. Such unique properties of direct-electrothermal heating result in a readily controllable effluent as it exits the adsorption vessel during regeneration.

Granular activated carbon (GAC) is the traditional morphology of activated carbon that is used to adsorb organic vapors from gas streams. GAC has a nominal diameter of 4–7 mm [16]. GACs are commercially available on a widespread basis with a nominal cost of $2/kg. However, activated carbons are now available with a wide range of morphologies that provide unique adsorption and regeneration properties. Commercially available activated carbons in the form of a monolith [ACM, 14,17], MAST monolith [18], activated carbon beads [ACB, 19], and ACFC [12] have been studied individually with respect to their unique properties to capture organic vapors from gas streams and allow for direct-electrothermal regeneration of the adsorbent. However, these materials have not yet been compared and contrasted in the literature. Such analysis is important because it better describes the physical, electrical and adsorption properties of adsorbents with specific morphologies that can be used to capture and recover organic vapors from gas streams.

1.1. Activated carbon adsorbents: monolith, bead, and fiber cloth

ACM described here is a coal-based adsorbent that is made with powdered activated carbon (PAC) that initially contains 4–6% by mass ash and a specific surface area of 900–1100 m^2/g [3]. PAC is mixed with water and an organic binder, and then extruded at high pressure, and dried between 400°C and 500°C to form a monolith. The ACM used in this study has the shape of a parallelepiped with length of 10 cm (Z) and square cross-section of 5 cm per side (L). The monolith contains 400 longitudinal parallel open channels of square section of 0.2 cm per side, and wall thickness between the channels of 0.05 cm. ACM has a nominal cost of $3.60/kg. The N_2 BET-surface area of the monolith is 603 m^2/g, it has a Dubinin–Radushkevich micropore volume of 0.21 cm^3/g, the volumetric mass density of the solid is 1.04 g/cm^3, the apparent density of the monolith is 0.37 g/cm^3, and its porosity is 0.64 (volume of channels/total volume of the monolith) [20]. Superficial gas velocities as high as 2 m/s can be treated in contrast to 0.1–0.6 m/s for GAC [3]. The gas stream enters through each of the channels and the organic vapor is transported into the walls of the channels and is adsorbed into the activated carbon (Fig. 1A). The clean gas stream then exits the monolith. The organized structure of the ACM channels allows for intimate contact between the gas stream and the monolith's walls. Overall, ACMs allow for relatively high adsorption capacity, small pressure drop, a compact system, and is suitable for treatment of high volumetric flow rates (e.g., 7×10^6 m^3/h) for gases with a wide range of organic vapor concentrations (e.g., 2–8 g/m^3), and stable catalytic combustion of the vapors [3].

ACB is a synthetic carbonaceous adsorbent, which contains a highly sulfonated styrene divinylbenzene resin, and is produced by pyrolysis and activation between 300 °C and 1200 °C. Pyrolysis and activation increases the microporosity of the beads, while only providing a small increase in the samples mesoporosity. The ACB adsorbent was produced commercially by Rohm and Hass (Ambersorb 572) with a mean particle diameter of 0.6 mm (Fig. 1B). The manufacturer reports that this material is less reactive than GAC toward components such as ketones, resulting in less risk of fires when using ACBs. ACB (Ambersorb 572) has a nominal cost of $1575/kg. Its N_2-BET specific surface area is 1100 m^2/g. The adsorbent's pore volume is 51% microporous, with micropore, mesopore, and macropore volumes of 0.41 cm^3/g, 0.19 cm^3/g, and 0.20 cm^3/g, respectively[19]. A unique aspect of ACBs is their potential use in fluidized bed adsorbers due to their small diameter, high adsorption capacity, and resistance to mechanical attrition with a crush strength >1 kg/bead [21,22].

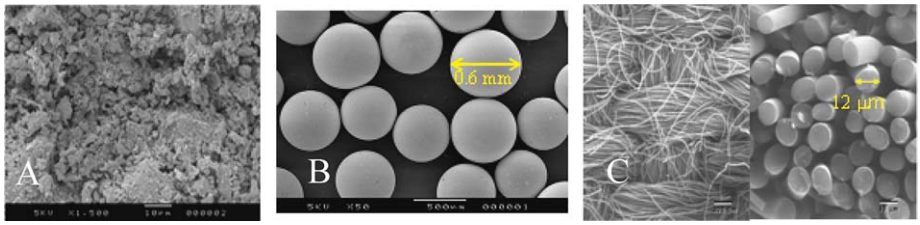

Fig. 1. Scanning electron microscope images of (A) ACM [19], (B) ACB [20] (Ambersorb 572), and (C) ACFC [26].

Activated carbon fibers (ACFs) are made from novoloid, pitch, cellulose, rayon, polyacrylonitrile and saran. ACFs are shapeable and can be formed as activated carbon fiber paper, activated carbon fiber felt, and ACFC. ACFCs' surface areas can range from 700 m^2/g to 2400 m^2/g, which provides larger surface areas than commonly used GACs [23]. ACFC used in this study is made from phenolic Novolac™ resin and is identified here as ACFC-5092-20 (Model ACC-5092-20, American Kynol Inc., Pleasantville, NY, Fig. 1C). ACFC-5092-20 has a nominal cost of $730/kg. The pores of ACFC are dominated by micropores (e.g., >93% by volume) with mean total pore width ranging from 7.4 to 9.9 and micropore pore width ranging from 6.9 Å to 9.8 Å, depending on the lot of ACFC tested [24,25]. ACFC's physical properties provide rapid adsorption and high adsorption capacities for a wide range of organic vapors [23,25]. Mass and heat transfer of vapors to and from the ACFCs are also enhanced because of their low nominal fiber diameter of 12 μm [25]. The ACFC used here has an N_2-BET surface area of 1604 m^2/g, electrical resistivity of 6×10^{-3} Ω m at 22 °C [25], and consists of 95.1% carbon, 0.4% hydrogen, 4.5% oxygen, <0.05% nitrogen, and 0% ash by mass, as determined by ultimate analysis [25]. Ash free adsorbents are useful to restrain unwanted chemical reactions and fires within the adsorption vessel that occur with typical GACs that contain ash. The shapeable woven ACFC readily permit the formation of annular and pleated cartridges. These unique properties make ACFC a desirable adsorbent for gas separation and air pollution control applications.

1.2. Chemical and physical properties of the adsorbate

Toluene (C_7H_8) is used as the adsorbate for each of the adsorption systems discussed here. Toluene is an important organic vapor because it is a hazardous air pollutant and 81×10^6 kg/yr of toluene is emitted to the atmosphere from USA [27]. Toluene is aromatic, with a molecular weight of 92.1 g/mole, molecular diameter of 6.95 Å, boiling point of 110.6 °C, dipole moment of 0.4 Debyes, liquid density of 0.87 g/cm^3 at 20 °C, and saturation vapor pressure of 22.0 torr at 20 °C [28].

2. Experimental methodology

2.1. Configurations and experimental procedures

The bench-scale ACM adsorption system consisted of a vapor generation system, an adsorption cell, a source of compressed N_2, a gas chromatograph, an electrical power supply, and a data acquisition and control system (Fig. 2). The vapor generator included two syringe pumps with hypodermic needles, an evaporator, a static gas mixer and a mass flow meter to control the N_2 gas flow rate. The concentration of the organic vapor in the gas stream was controlled by the flow rate of N_2 and of the liquid feed rate of the organic compound.

The adsorption cell consisted of a Teflon jacket that supported the ACM (Fig. 3A). A removable flat cover was used to close the cavity. Two sheets of graphite paper were located between flat-plate copper electrodes and the opposing surfaces of the monolith to provide a uniform electrical circuit with the ACM. Six screws were used to press the copper plates, graphite paper, and monolith together. The electrical leads passed through the Teflon enclosure and were welded onto the copper plates. There was 93.6 g of ACM in a cell that had a bulk cross-sectional area of 25 cm^2 and a length of 10 cm. The system was electrically insulated and waterproofed. The temperature of the monolith was measured with a Pt probe that was positioned at the exit of the middle channel of the ACM.

The total gas flow rate during an adsorption test was 3.2 L/min (at 20 °C and atmospheric pressure). Concentration of the gas stream at the outlet of the adsorption cell was monitored with a gas chromatograph with a flame ionization detector (FID). Prior to each adsorption run, the gas stream was prepared, directed off-line and monitored by gas chromatography until the selected organic vapor concentration remained stable for 60 min. The gas stream was then directed to the adsorption cell by switching a

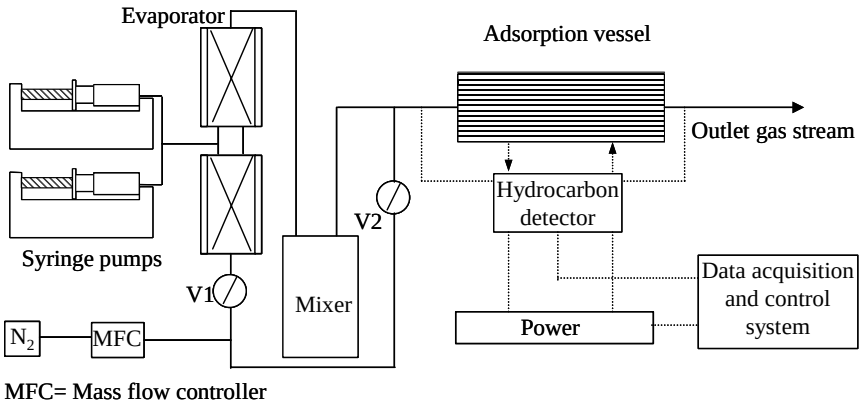

Fig. 2. General schematic of the experimental apparatus for ACM, ACB, and ACFC systems.

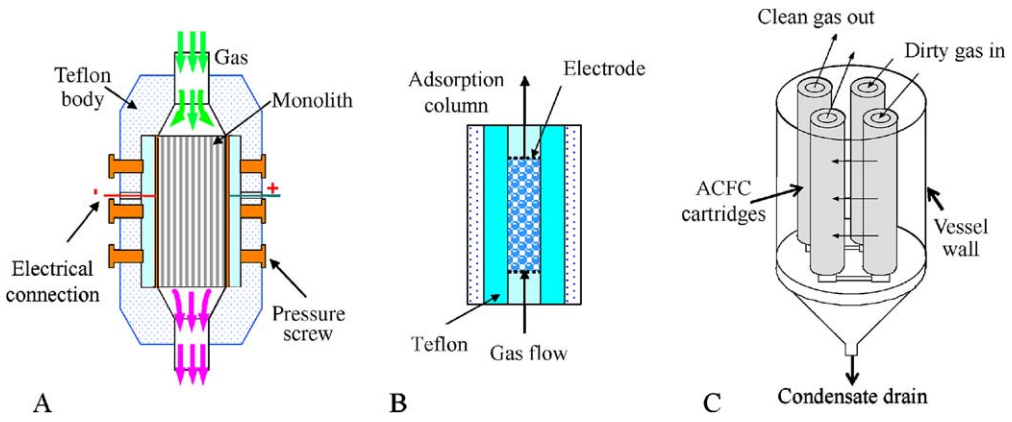

Fig. 3. Schematic of the (A) ACM [13], (B) ACB, and (C) ACFC adsorption vessels (adapted from reference [12]).

three-way valve. The organic vapor concentration was then detected downstream of the adsorption cell. The adsorption cell was then saturated with the organic vapor, taken off-line, and then regenerated with direct-electrothermal regeneration. The cell was purged with 1.6 L/min of N_2 (20 °C and atmospheric pressure) during regeneration to assure passage of the vapors from the adsorption column during regeneration. Electrothermal regeneration of the ACM and N_2 flow through the adsorption column started simultaneously. The electric current intensity was kept constant during regeneration, with voltage depending on the monolith's electrical resistance.

The bench-scale ACB adsorption system consisted of a vapor generation system, an adsorption column, a source of compressed N_2, a gas chromatograph, an electrical power supply, a gravimetric balance, and a data acquisition and control system (Fig. 2). The N_2 flow rate to the adsorption column was controlled with mass flow controllers. Liquid toluene was injected into one of the gas streams using a hypodermic needle, a syringe pump, and an evaporator to mix the vapor with the N_2 at ambient pressure. The solvent-laden gas stream then mixed with additional N_2 and then fed into the fixed adsorption at a flow rate of 1 L/min (at 20 °C and 1 atm). There was 3.5 g of ACBs located in the Teflon adsorption column that had an inner diameter of 1.6 cm and a length of 3.5 cm (Fig. 3B). The effluent concentration was determined using a gas chromatograph with an FID as used with the ACM tests. Electrothermal desorption of the ACBs occurred once the adsorbent was saturated with organic vapor. N_2 flowed through the column as electricity passed through the ACBs. A constant electrical current was applied to the electrodes during each regeneration cycle as with the ACM regeneration tests.

The experimental apparatus for the bench-scale ACFC adsorption system consisted of an organic vapor generator, an inlet high efficiency particulate air filter, two adsorption vessels, a source of compressed N_2, a total hydrocarbon detector, and a data acquisition and control system (Fig. 2).

Air passed through the organic vapor generator while liquid toluene was injected into the gas stream using a hypodermic needle and a syringe pump. A small piece of ACFC was wrapped around the hypodermic needle to allow for more uniform evaporation of the toluene into the gas stream. The flow rate of air was controlled with mass flow controllers. The concentration of organic vapor was measured with a photoionization detector (PID, Rae Systems Inc., Model ModuRae) or a FID (MSA/Baseline Inc., series 8800). The organic vapor-laden air stream passed through a cylindrical, stainless-steel or aluminum adsorption vessel that contained four annular cartridges of ACFC to adsorb the organic vapor from the air stream (Fig. 3C). The bench-scale system contained 151 g of ACFC per vessel that provided eight layers of cloth for each cartridge. Nominal total gas flow rate for the system was 100 L/min (at 0 °C and 1 atm). Once breakthrough occurred, N_2 flowed through the vessel at 1% of the gas flow rate that was experienced during the adsorption cycle to purge O_2 from the vessel before the ACFC was regenerated, and to assist with the flow of organic vapor from the vessel as it desorbed from the ACFC. The resulting concentrated vapor condensed onto the interior walls of the vessel's base, drained from the base of the vessel into a reservoir, and was then measured with a gravimetric balance [29].

2.2. Pressure drop, permeability, throughput ratio, length of unused bed, and electrical resistivity

Pressure drop for the ACM and ACB adsorption systems was determined with the following equation [19]:

$$\Delta P = \frac{32 Z \mu u}{d_h^2} \quad (1)$$

where ΔP = pressure drop, Z = adsorption bed length, μ = gas viscosity; u = superficial gas velocity; d_h = adsorbent's hydraulic diameter determined as follows:

$$d_h = 4(\text{void volume})/\text{surface area} \quad (2)$$

which results in d_h = ACM channel's side length for the ACM system. However, for the ACB system,

$$d_h = \frac{2\varepsilon}{3(1-\varepsilon)} d_b \tag{3}$$

where ε = apparent porosity of the ACBs in the adsorption vessel, and d_b = diameter of an ACB [19].

Pressure drop for the ACFC adsorption system was measured at the vessel's inlet at select gas flow rates using a U-tube manometer filled with water (Mod. 1222-8-W/M, Dwyer Inc.). Net pressure drop caused by the ACFC cartridge was determined by subtracting the pressure drop of the vessel without the ACFC adsorbent from the pressure drop of the vessel while containing the ACFC cartridge.

Permeability is a fluid flow parameter than characterizes the flow of gases through the ACM, ACB and ACFC adsorbents [30]. The pressure drop (ΔP) through the ACM and ACB adsorption systems can also be expressed as [31]:

$$\Delta P = \left(\frac{\rho_a C L}{2}\right) u^2 + \left(\frac{\mu_a L}{\alpha_p}\right) u \tag{4}$$

where ρ_a = air density, C = inertial resistance factor, L = adsorbent's length, μ_a = air viscosity, and α_p = permeability. Values of α_p and C are determined by linear regression with pressure drop data. Pressure drop for the ACFC system in the radial direction across the ACFC cartridges is as follows [31]:

$$\Delta P = \left[\frac{\rho_d C}{8\pi^2 L^2}\left(\frac{1}{r_i} - \frac{1}{r_o}\right)\right] Q^2 + \left[\frac{\mu_a}{2\alpha_p \pi L} \ln\left(\frac{r_o}{r_i}\right)\right] Q \tag{5}$$

where r_i = inner radius of the cartridge, r_o = outer radius of the cartridge, and Q = gas flow rate through each cartridge.

Values for throughput ratio (TPR) and the length of unused bed (LUB) were calculated to assess the performance of the system during an adsorption cycle. Higher TPR values indicate a steeper breakthrough curve, where transient mass-transfer limitations become less important. As TPR approaches unity, the time needed for the mass transfer zone to develop becomes insignificant compared to the time needed to saturate the adsorbent. TPR is expressed as $t_{5\%}/t_{50\%}$ where $t_{5\%}$ = time required to achieve 5% breakthrough and $t_{50\%}$ = time required to achieve 50% breakthrough. LUB describes the effective fraction of the adsorbent that is not utilized when the adsorption cycle is stopped at 5% breakthrough. LUB is expressed as 1- ($m_{5\%}/m_{100\%}$), where $m_{5\%}$ = mass of the organic vapor adsorbed at time $t_{5\%}$ and $m_{100\%}$ = mass of the organic vapor adsorbed when the adsorbent is saturated.

Electrical resistivity ($\rho_{r,o}$) is an intrinsic parameter that can be used to characterize the ACM, ACB, and ACFC. This parameter is dependent on the temperature, precursor, and degree of activation. The general equation describing $\rho_{r,o}$ for a homogeneous conductor at a reference temperature (T_R) is defined as [32]:

$$\rho_{r,o} = \left(\frac{A}{L}\right) R \tag{6}$$

where A = cross-sectional area perpendicular to the current flow, R = electrical resistance, and L=length parallel to the current flow.

Resistivity dependence on temperature is described by [32]:

$$\rho_r(T) = \rho_{r,o}(1 + \alpha_r(T - T_R)) \tag{7}$$

where T = adsorbent's temperature and α_r = thermal resistivity factor. Parameter α_r is obtained by linear regression of the adsorbent's electrical resistance at select temperatures.

The ACM, ACB, and ACFC adsorbents are heterogeneous due to the voids caused by the channels within the ACM, around each ACB, and between the individual ACFs. The electrical resistivity is related to the electrical resistance (R) for the ACM by considering the monolith as a combination of basic cells in parallel and/or series as described below [19]:

$$\rho_r = RZ\left(1 + \frac{\varepsilon}{1 - \sqrt{\varepsilon}}\right)^{-1} \tag{8}$$

Resistivity for the ACB was determined by considering the resistance of a bead and the resistance of contact between two vertically adjacent beads, as described below [19]:

$$\rho_r = \rho_{bead,eff} + \rho_{contact,eff}(p_{app})^{-\delta}. \tag{9}$$

Where $\rho_{bead,eff} = R_b d_b$ with R_b = bead's electrical resistance,

$$\rho_{contact,eff} = \frac{K_2 d_b^2}{Z} \tag{10}$$

and p_{app} = pressure applied to the adsorbent to improve the electrical contact among the beads, $\delta = 0.2$ [19], and K_2 = coefficient factor between the electrical resistance of contact and the applied pressure.

$$K_2 = R^i_{contact} f_i^{\delta} \tag{11}$$

where $R^i_{contact}$ = electrical resistance between two beads at section element i, and

$$f_i = p_{app} + (i-1)\beta d_b \tag{12}$$

$(i-1)$ = section element within the adsorption vessel, and β = bead's apparent density within the adsorption vessel.

The electrical resistance for ACFC was determined by considering the effective ACFC thickness that is calculated by dividing the areal mass density of the bulk ACFC (ρ_a) with the true mass density of the fiber (ρ_t) [23]:

$$H_{eff} = \frac{\rho_a}{\rho_t} \tag{13}$$

This effective thickness represents the thickness of a hypothetically homogeneous (no interyarn and intrayarn void

volumes) sheet of ACFC. The effective cross-sectional area (A_{eff}) is then defined as [23]:

$$A_{eff} = WH_{eff} \tag{14}$$

where W = width of the ACFC perpendicular to the current flow. Electrical resistivity for the ACFC sample is then determined by replacing A with A_{eff}:

$$\rho_r = \left(\frac{A_{eff}}{L}\right)R \tag{15}$$

3. Results and discussion

Results that compare and contrast ACM, ACB, and ACFC electrothermal–swing adsorption systems are provided below. The properties used to describe these systems include their pressure drop, permeability, adsorption isotherm, breakthrough curve, TPR, LUB, electrical resistivity, and concentration factor obtained during electrothermal regeneration of the adsorbents when using toluene as the adsorbate.

3.1. Dependence of pressure drop and permeability for ACM, ACB, and ACFC

Dependence of pressure drop per unit length of adsorbent on superficial gas velocity for the ACM, ACB, and ACFC adsorbents indicates a linear dependence of pressure drop on gas velocity (Fig. 4). As expected the monolith had the smallest pressure drop with its well designed open channels.

Permeability values for the ACM, ACB, and ACFC systems are 1.76×10^{-8} m^2, 1.98×10^{-10} m^2, and 1.92×10^{-11} m^2, respectively. This results in a gas stream flowing easier through the ACM when a pressure gradient is applied to the system. Permeability values for ACM, ACB, and ACFC range over three orders of magnitude, but are in the range of typical permeability values for porous materials ranging from Berl saddles (2.6×10^{-7} m^2) to sandstone (1.5×10^{-12} m^2) [30, Table 1].

Table 1
Physical, Electrical, Adsorption, and Cost Properties of ACM, ACB, and ACFC

Adsorbent	ACM	ACB	ACFC
Pressure drop at 0.1 m/s of Superficial gas velocity (Pa/cm)	1.0	89.9	38.8
Permeability (m^2)	1.8×10^{-8}	2.0×10^{-10}	1.9×10^{-11}
Micropore volume (cm^3/g)	0.21	0.41	0.75
Adsorption capacity at $p/p_o = 0.9$ (g/g)	0.26	0.52	0.6
Throughput ratio	0.81	0.91	0.81
Length of unused bed	0.21	0.08	0.21
Electrical resistivity at 455 K ($\Omega - m$)	3.9×10^{-1}	8.1×10^{-2}	4.8×10^{-3}
Max. achieved concentration factor	46	20	1050
Cost ($/kg)	3.6	1,575	730

3.2. Equilibrium adsorption isotherms for toluene vapor with ACM, ACB, and ACFC Adsorbents

Adsorption isotherm results are important to determine the maximum organic vapor partitioning that can occur for each adsorbent, assuming no mass transfer limitations of the unit operation. The ACM, ACB, and ACFC exhibit a Type I isotherm up to p/p_o of 0.8 due to the micropores existing in the adsorbents (Fig. 5). ACFC has 400% and 67% larger adsorption capacity at lower relative pressures ($\leqslant$0.2 p/p_o, where p = actual vapor pressure, and p_o = saturation vapor pressure) when compared to the ACM and ACB, respectively. However, the adsorption capacities of ACFC and ACB approach each other at larger p/p_o values ($\geqslant$ 0.9 p/p_o), while the adsorption capacity of the ACM is limited to 50% of the adsorption capacity for the ACFC and ACB at the same elevated vapor concentration. The lower adsorption capacity of ACM is caused by its smaller specific pore volume, probably due to its binder and ash content.

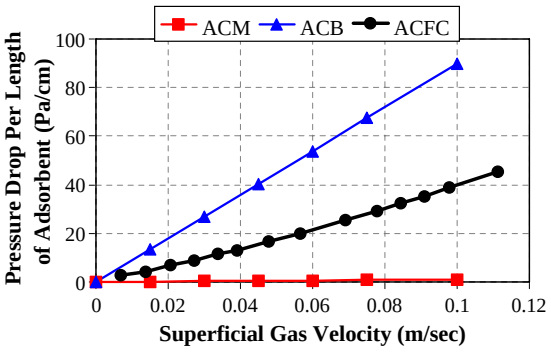

Fig. 4. Dependence of pressure drop per unit thickness of adsorbent on superficial gas velocity for ACM, ACB, and ACFC.

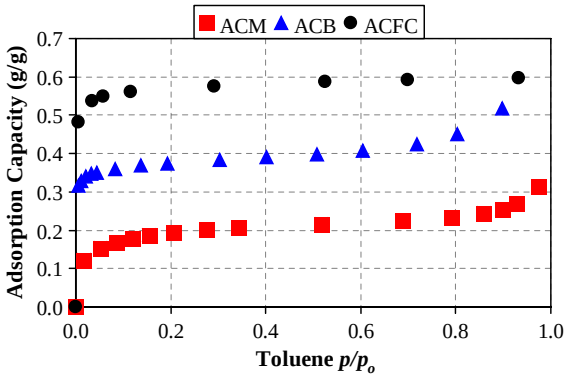

Fig. 5. Comparison of adsorption isotherms for toluene with ACM, ACB, and ACFC adsorbents at 20 °C and atmospheric pressure.

3.3. Breakthrough tests for toluene vapor and ACM, ACB and ACFC adsorbents

Dimensionless breakthrough tests for ACM, ACB, and ACFC describe the change in the ratio of the toluene vapor concentrations at the outlet to the inlet of the adsorption vessel during an adsorption cycle (Fig. 6). The concentration ratio is plotted as a function of another ratio, which is the duration of the adsorption cycle divided by $t_{50\%}$. Such format allows comparison of the structure of the breakthrough curves under a wide range of inlet vapor concentrations, masses of adsorbent in the adsorption vessels, and gas flow rates. The inlet toluene concentration for the ACM and ACB systems was 1300 ppmv (5 g/m^3 at 20 °C and 1 atm), while the inlet concentration for the ACFC system was 680 ppmv (2.6 g/m^3 at 20 °C and 1 atm). The superficial gas velocities for the adsorption of toluene by the ACM, ACB, and ACFC adsorbers were 3.2 cm/s, 3.3 cm/s, and 8.4 cm/s, respectively.

TPR/LUB values for the ACM, ACB, and ACFC are 0.81/0.21, 0.91/0.08, and 0.81/0.21, respectively. A minimum TPR value of 0.7 and a maximum acceptable LUB value of 0.3 have been proposed as acceptable guidelines [23]. TPR and LUB values for the adsorption systems studied here were all acceptable within the stated guidelines. Such results indicate that the ACM, ACB and ACFC adsorbent materials were effectively utilized to capture toluene from the gas streams at the specified conditions.

3.4. Electrical resistivity dependence on temperature for ACM, ACB, and ACFC

Electrical resistivity for ACM, ACB, and ACFC between 280 K and 540 K are provided in Fig. 7. The dependence of resistivity on temperature and morphology of the adsorbents is provided because the temperature of the adsorbent can increase by more than 200 °C during electrothermal regeneration and the morphologies of the studied adsorbents are distinctly different. All of the adsorbents exhibited a decrease in resistivity with increasing temperature. This is typical of carbonaceous materials, which are semi-conductors. The arithmetic mean thermal resistivity factor (α_r) is -3×10^{-3} K^{-1} for all three materials, which is also representative of semi-conductors. Linear regressions for each material yielded arithmetic mean (standard deviation) values for α_r of -2.68×10^{-3} K^{-1} (2.0×10^{-4}), -2.72×10^{-3} K^{-1} (1.1×10^{-3}), and -3.62×10^{-3} K^{-1} (1.8×10^{-3}) for ACM, ACB and ACFC, respectively. ACM has the highest resistivity values, which is probably due to the degree of carbonization for the binder. The relatively high resistivity values for ACB is most likely due to the resistivity of the contacts that exist between beads in the vessel, as demonstrated by the decrease in resistivity with increasing amount of compression for the ACBs [19].

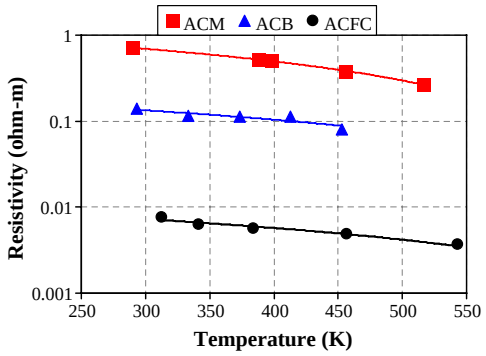

Fig. 7. Electrical resistivity dependence on temperature for ACM, ACB and ACFC adsorbents.

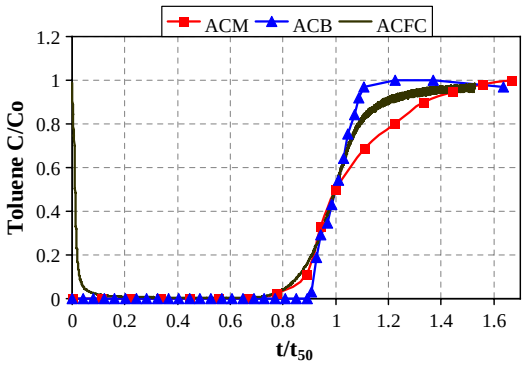

Fig. 6. Dimensionless breakthrough curves for toluene with ACM, ACB, and ACFC adsorbents.

3.5. Concentration factors during desorption for ACM, ACB, and ACFC

Direct-electrothermal regeneration of ACM, ACBs, and ACFC allows for careful control of the outlet concentration of the organic vapor during regeneration of the adsorbent. Such careful control of the outlet concentration is very difficult with steam, hot gas, and vacuum regeneration because of the difficulties in controlling the energy applied to the adsorbent separately from the carrier gas flow rate. Electrothermal regeneration can readily control the energy deposited to the adsorbent separate from the carrier gas flow rate during the regeneration cycle. Such approach is important when using adsorption to capture and recover organic vapors [11,12] or to capture, concentrate and then destroy organic vapors that do not have sufficient economic value or purity to allow for re-use.

The concentration factor (C/C_o) describes the ratio of the organic-vapor concentration at the outlet of the adsorption column during the regeneration cycle to the organic-vapor concentration at the inlet of the adsorption vessel during the adsorption cycle (Fig. 8). The inlet toluene concentration for the ACM and ACB systems was 1300 ppmv (5 g/m^3 at 20 °C and 1 atm), while the inlet concentration for the ACFC system was 680 ppmv (2.6 g/m^3 at

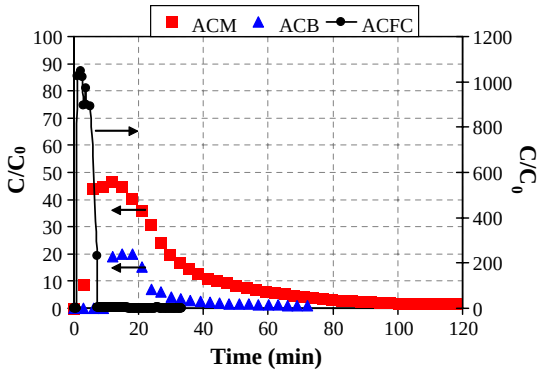

Fig. 8. Concentration factors for toluene with ACM, ACB, and ACFC adsorbents.

20 °C and 1 atm). The superficial gas velocities of N_2 during the desorption of toluene with the ACM, ACB, and ACFC systems were 1.67 cm/s, 4.14 cm/s, and 0.06 cm/s, respectively. The ACM and ACB were regenerated while preventing the condensation of toluene in the exhaust gas stream. However, the ACFC was regenerated with the intent to provide toluene condensate without the use of any auxiliary heat exchangers. Electrothermal heating tests for the ACM without adsorbate indicated that the monolith can be readily heated to 200 °C within 8 min. This test would have provided high C/C_o values, if the test was performed with saturated adsorbent. These results demonstrate how carefully controlled concentration factors can be readily achievable when the energy applied to the adsorbent is controlled rapidly and separately from the carrier-gas flow rate during the electrothermal regeneration cycle.

4. Summary and conclusions

Activated carbons in the form of a monolith (ACM), beads (ACBs), and fiber cloth (ACFC), which can be treated with direct-electrothermal heating, were characterized with respect to pressure drop, permeability, adsorption capacity, breakthrough curve, throughput ratio (TPR), length of unused bed (LUB), electrical resistivity, concentration factor during regeneration, and cost (Table 1). It was imperative to carefully consider the morphologies of each adsorbent when comparing these properties. Each adsorbent had its own set of attributes when considering the application of these adsorbents to capture and recover organic vapors from gas streams when using electrothermal–swing adsorption.

ACM had 1% and 3% of the pressure drop at 0.1 m/s of superficial gas velocity when compared to ACB and ACFC, respectively, for the bench-scale tests described here. ACM's permeability was 2 and 3 orders of magnitude larger than for ACB and ACFC, respectively. ACM's morphology allowed a much less tortuous path for the gas resulting in the largest permeability and lowest pressure drop. Pressure drop and permeability are important design properties when considering operating costs for the system. ACFC had on average 205% and 46% larger adsorption capacity for toluene than ACM and ACB, respectively. ACFC's larger adsorption capacity is attributed to its larger specific surface area and micropore volume when compared to ACM and ACB. Dimensionless breakthrough curves for ACM, ACB, and ACFC showed similar profiles regardless of the tested inlet toluene concentration and superficial gas velocity. TPR and LUB values for ACM, ACB and ACFC proved that these novel morphologies were effective at capturing toluene vapor for the conditions tested here.

ACFC had 1–2 orders of magnitude lower electrical resistivity at 455 K, and was at least 5–10 times faster to regenerate up to a C/C_o value of 4 when compared to ACB and ACM, respectively. ACFC's concentration factor was more than 22 times the concentration factor for ACM and ACB. Electrothermal regeneration of ACM, ACB, and ACFC provided a wide range of readily controllable concentration factors at the outlet of all three systems. Such control of concentration factors is readily achievable because the energy applied to the adsorbent is controlled rapidly and separately from the carrier-gas flow rate during the electrothermal regeneration of the adsorbents.

Acknowledgement

This research was supported by UIUC/CNRS Cooperative Research Program, Grainger Foundation, U.S. National Science Foundation (DMI-02-17491), and CONACYT-Mexico.

References

[1] Benson RE, Courouleau PH. European practice for solvent recovery in printing industry. Chem Eng Progress 1948;44(6):459–68.
[2] Rafson HJ. Odor and VOC control handbook. New York: McGraw-Hill; 1998.
[3] Qiao H. Research Institute of Chemical Defense technical report. Beijing, China, 1989;7.
[4] Ruthven DM. Principles of adsorption and adsorption processes. New York: Wiley; 1984.
[5] Guerin P, Domine D. Process for separating a binary gas mixture by contact with an adsorbent. French patent 1233261, 1957.
[6] Hauck W, Grevillot G, Lamine AS. Induktionsheizung: Anwendung auf die Regenerierung von beladenen Aktivkohle Festbetten. Chemie Ing Techn 1997;69(8):1138–42.
[7] Mocho P, Bourhis JC, Le Cloirec P. Heating activated carbon by electromagnetic induction. Carbon 1996;34(7):851–6.
[8] Petkovska M, Tondeur D, Grevillot G, Granger J, Mitrovic M. Temperature swing gas separation with electrothermal desorption step. Sep Sci Technol 1991;26(3):425–44.
[9] Baudu M, Le Cloirec P, Martin G. Thermal regeneration by Joule effect of activated carbon used for air treatment. Environ Technol 1992;13(5):423–35.
[10] Subrenat A, Le Cloirec P. Adsorption onto activated carbon cloths and electrothermal regeneration: its potential industrial applications. J Environ Eng 2004;130(3):249–57.
[11] Lordgooei M, Sagen J, Rood MJ, Rostam-Abadi M. Sorption and mass transfer of toxic chemical vapors in activated carbon fiber cloth fixed-bed adsorbers. Energy Fuels 1998;12(6):1079–88.

[12] Sullivan PD, Rood MJ, Grevillot G, Wander JD, Hay KJ. Activated carbon fiber cloth electrothermal swing adsorption system. Environ Sci Technol 2004;38(18):4865–77.
[13] Dombrowski KD, Lehmann CMB, Sullivan PD, Ramirez D, Rood MJ, Hay KJ. Solvent recovery and energy efficiency during electric regeneration of an ACF adsorber. J Environ Eng 2004;130(3):268–75.
[14] Yu F, Luo L, Grevillot G. electrothermal desorption using Joule effect on an activated carbon monolith. J Environ Eng 2004;130(3): 242–8.
[15] Cheng ZM, Yu F, Grevillot G, Luo L, Yuan WK, Tondeur D. Redistribution of adsorbed VOCs in activated carbon under electrothermal desorption. AIChE J 2002;48(5):1132–8.
[16] Smísek M, Cerný S. Active carbon: manufacture, properties and applications. Czechoslovakia: Elsevier Pub Co; 1970.
[17] Yu F, Luo L, Grevillot G. Adsorption isotherms of VOCs onto monolith activated carbon: experimental measurement and correlation with different models. J Chem Eng Data 2002;47(3):467–73.
[18] Tennison S, Blackburn A, Rawlinson T, Place R, Crittenden B, Perera S, et al. Electrically regenerable monolithic adsorption system for the recovery and recycle of solvent vapours. In: eighth fundamental of adsorption. Sedona (Arizona. USA): 2004. p. 22–8.
[19] Saysset S. Procédé d'adsorption sur adsorbant carboné avec régénération thermique par effet Joule direct. Application au traitement d'effluents chargés en composés organiques volatils. Lorraine Nancy France, L'Institut National Polytechnique de Lorraine, Ph.D. thèses, 1999.
[20] Yu F. Adsorption of organic volatile compounds with activated carbon monolith with electrothermal regeneration using the Joule effect. Lorraine Nancy France, L'Institut National Polytechnique de Lorraine, Ph.D. thèses, 2003.
[21] Duan W, Song WL, Luo L. Experimental study on VOCs adsorption in a two-stage circulating fluidized bed. Chinese J Process Eng 2004; 4(3):210–4.
[22] Song W, Tondeur D, Luo L, Li J. VOC adsorption in circulating gas fluidized bed. Adsorption 2005;11(1):853–8.
[23] Sullivan PD, Rood MJ, Hay KJ, Qi S. Adsorption and electrothermal desorption of hazardous organic vapors. J Environ Eng 2001;127(3): 217–23.
[24] Hsi HC, Rostam-Abadi M, Rood MJ, Chen S, Chang R. Effects of sulfur impregnation temperature on the properties and mercury adsorption capacities of activated carbon fibers. Environ Sci Technol 2001;35(13):2785–91.
[25] Lo SY, Ramirez D, Rood M J, Hay KJ. Characterization of the physical, thermal and adsorption properties of a series of activated carbon fiber cloths. In: Proceedings of the air and waste management's 95th annual conference and exhibition. Baltimore, Maryland, USA: Air and Waste Management Association, 2002.
[26] Lo SY. Characterization of the chemical, physical, thermal and electrical properties of a series of activated carbon fiber cloths. Urbana, IL, USA, University of Illinois at Urbana-Champaign, Master thesis, 2000.
[27] USEPA. EPA air pollution control cost manual. Research Triangle Park NC: US Environmental Protection Agency, 2002.
[28] Reid RC, Prausnitz JM, Poling BE. The properties of gases and liquids. 4th ed. New York: McGraw-Hill; 1987.
[29] Emamipour H, Kaldate A, Rood MJ, Thurston D. Experimental study of cyclic adsorption/desorption of MEK in an ESA device. In: Proceedings of the air and waste management's ninety-eighth annual conference and exhibition. Minneapolis, Minnesota, USA): Air and Waste Management Association; 2005.
[30] Collins RE. Flow of fluids through porous materials. New York: Reinhold Publishing Co.; 1961.
[31] FLUENT Version 6.0 User's Guide Volumes 1 and 2: FLUENT Inc.; 2001.
[32] Lindeburg MR. EIT review manual. San Carlos, CA: Professional Publications; 1982.